# TRANSGRANULAR SLITS IN ALUMINUM INTERCONNECTS CAUSED BY THERMAL STRESS AND ELECTRIC CURRENT

W. WANG, Z. SUO AND T.-H. HAO*
Mechanical Engineering Department, University of California, Santa Barbara, CA 93106.
*On leave from China Textile University, Shanghai 200051, P.R. China.

## ABSTRACT

An aluminum interconnect can fail by a transgranular slit. We show how a rounded void collapses to such a slit, as atoms diffuse on the void surface, driven by electric current, thermal stress, and surface energy. We use a variational principle to simulate the shape evolution, and identify the critical conditions to trigger the shape instability.

## INTRODUCTION

In accelerated tests, aluminum interconnects are subjected to intense electric current (~ $10^{10}$ A/m$^2$), high thermal stress (~ 400 MPa), and absolute temperature exceeding a half of the melting point (933K). Transgranular slits have been observed in single crystal and bamboo-like lines [1-4]. So far little consensus has been reached on why these slits form [5]. Here we report our recent simulations of void instability due to surface diffusion under thermal stress or electric current. Crystalline anisotropy, especially in surface energy and surface diffusivity, plays roles in the instability. However, to focus on other important aspects of the problem, we assume that the conductor is isotropic. Material properties to be used in estimations are listed in Table I.

## INSTABILITY UNDER STRESS

A rounded void under sufficiently high stress will collapse to a slit as atoms diffuse from one portion of the void surface to another [7-9]. Figure 1 illustrates a cylindrical void in an infinite crystal under biaxial stress $\sigma_1 = \sigma_2 = \sigma$. A circular void is in equilibrium: no force drives diffusion. Yet this equilibrium can be unstable. When the void is perturbed to become, say, an ellipse, atoms will diffuse on the void surface, leading to further change in the void shape. Surface energy will strive to restore the circular symmetry by driving atoms to diffuse from B to A. On the other hand, the elastic energy density at A is larger than that at B; the stress will strive to amplify the asymmetry by driving atoms to diffuse from A to B. The void collapses if the elastic energy dominates over the surface energy. Let $a_0$ be the radius of the circular void, $\gamma_s$ the surface energy, and $Y$ Young's modulus. The capillary effect scales as $\gamma_s/a_0$, and the strain energy density scales as $\sigma^2/Y$. The relative magnitude of the two competing forces defines a dimensionless number

Table I Pure Aluminum Data

| | |
|---|---|
| Atomic volume | $\Omega = 1.66\times10^{-29}$ m$^3$ |
| Young's modulus | $Y$= 70 GPa |
| Surface diffusivity | $D_s = 10^{-5}\times\exp[-0.7(\text{ev})/kT]$ m$^2$/s [6] |
| Effect surface thickness | $\delta_s = 2.86\times10^{-10}$ m (approximated by the Burgers vector) |
| Surface energy | $\gamma_s$ = 1 J/m$^2$ |
| Effective valence | $Z_s^* = 20$ |



Mat. Res. Soc. Symp. Proc. Vol. 338. ©1994 Materials Research Society

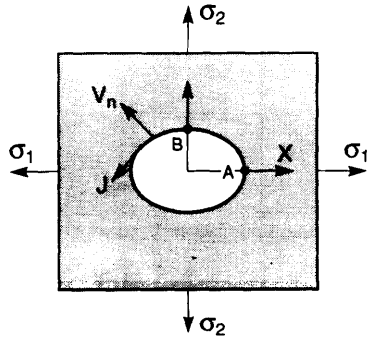


Fig. 1 A cylindrical void in an infinite elastic solid under biaxial stresses.

$$\Lambda = \frac{\sigma^2 a_0}{\gamma_s Y}. \tag{1}$$

When $\Lambda$ is small, surface energy dominates, and the void will relax to a circle. When $\Lambda$ is large, strain energy dominates, and the void will collapse to a slit. For a circular void under the equal biaxial stress, the critical number is found to be $\Lambda_c = 3/8$. The stability of the void depends on both the applied stress and the void size. Under thermal stress $\sigma$ = 300 MPa, the critical void radius is $a_0 = 0.29$ $\mu$m. Biased stress does not change the instability condition very much [8].

The instability is better understood by viewing the potential energy landscape. Under fixed load, the suitable potential is $\Phi = (\text{Surface Energy}) + (\text{Strain Energy}) - (\text{Load}) \times (\text{Displacement})$. For linear elastic solids, $(\text{Strain Energy}) = (1/2)(\text{Load}) \times (\text{Displacement})$. Thus,

$$\Phi = (\text{Surface Energy}) - (\text{Strain Energy}). \tag{2}$$

Atoms diffuse on the void surface to reduce the potential, causing the void to change shape but conserve volume. Both the surface energy and the strain energy will increase when a circular void changes to any other shapes. The potential will be reduced if the surface energy increases less than the strain energy. We approximate the void shape by a family of ellipses. Let $\Delta\Phi$ = $\Phi$(ellipse) - $\Phi$(circle), $a$ and $b$ be the semi-axes, and $m = (a-b)/(a+b)$ describe the shape. The circle corresponds to $m = 0$, the $x$-direction slit to $m \to +1$, and the $y$-direction slit to $m \to -1$.

Figure 2 displays the potential as a function of the void shape at several constant levels of $\Lambda$. Each minimum and maximum represents a stable and unstable equilibrium state, respectively. Three behaviors are possible depending on the value of $\Lambda$. (1) When $\Lambda = 0$, no stress is applied; $\Phi$ reaches a minimum at $m = 0$, and maxima at $m = \pm 1$. The circular void is stable and the two slits are unstable: any ellipse will relax to the circle. (2) When $\Lambda \in (0, 3/8)$, the stress is finite but surface energy still dominates; $\Phi$ reaches a local minimum at $m = 0$, two maxima at some $\pm m_c$, and two minima at $m = \pm 1$. The maxima act as energy barriers: an ellipse of $|m| < m_c$ will relax to the circle, but an ellipse of $|m| > m_c$ will collapse to the slits. (3) When $\Lambda \in (3/8, \infty)$ the stress dominates; $\Phi$ reaches the maximum at $m = 0$, and minima at $m = \pm 1$. The circle is unstable but the slits are stable: any elliptic void will collapse to the slits.

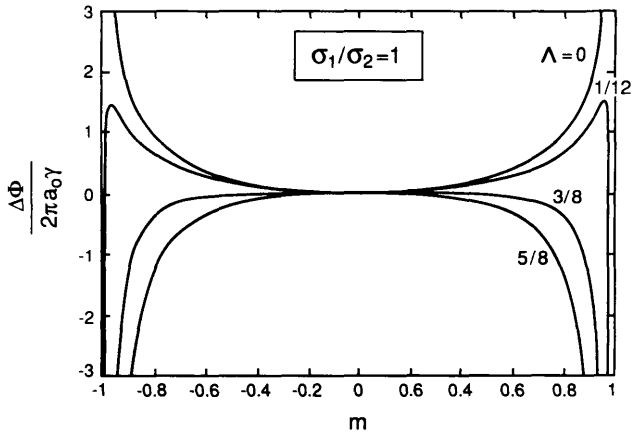


Fig. 2 The potential as a function of shape factor $m$ at several levels of $\Lambda$.

Shape evolution was simulated as follows [8]. At any fixed time $t$, the position vector $\mathbf{x}$ on the surface is expressed as a function of a parameter $\theta$, i.e. $\mathbf{x} = \mathbf{x}(\theta, t)$, $0 < \theta < 2\pi$. For example, an ellipse is described by $x = a\cos\theta$ and $y = b\sin\theta$, with $a$ and $b$ evolving with the time. Denote $dl$ as the arc element and $\mathbf{n}$ the normal vector. The surface velocity is given by $V_n = \mathbf{n}\cdot\dot{\mathbf{x}}$. The superimposed dot represents the time rate. Denote $J$ as the atomic flux on the surface, i.e. the number of atoms per time crossing unit length on the surface. Mass conservation requires that the velocity be related to the *divergence* of the flux, namely

$$V_n = \Omega \partial J / \partial l, \tag{3}$$

where $\Omega$ is the volume per atom.

A nonequilibrium void will change shape, by means of surface self-diffusion, to *decrease* the potential, i.e. $\dot{\Phi} < 0$. Define the force per atom that drives diffusion, $F$, such that

$$\dot{\Phi} + \int FJdl = 0 \tag{4}$$

for arbitrary virtual velocity and flux that conserve mass via (3). The integral extends over the void surface. This equation may also be interpreted as energy balance, the first term being the free energy rate ($\leq 0$), and the second the dissipation rate ($\geq 0$).

Following the usual kinetic law, we assume that the flux is linearly proportional to the force:

$$J = MF, \tag{5}$$

where $M$ is the mobility and is related to the diffusivity by the Einstein relation $M = D_s\delta_s / \Omega kT$, with $kT$ playing the usual role.

To ease numerical simulation, we formulated a variational principle to replace (4) and (5). Of all virtual flux and velocity that conserve mass via (3), the actual ones minimize the functional

$$\Pi = \dot{\Phi} + \int \frac{J^2}{2M} dl. \tag{6}$$

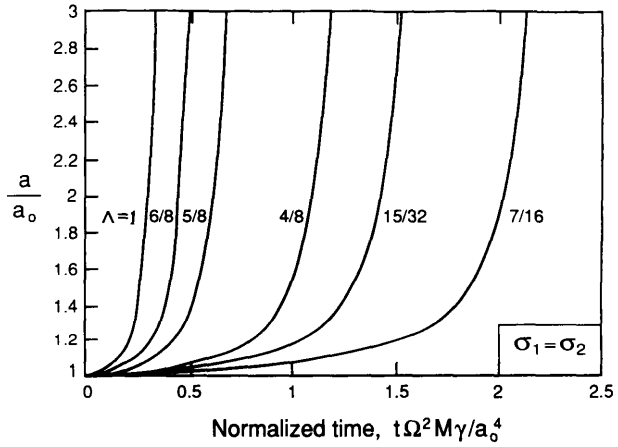


Fig. 3 The time for one ellipse to evolve to another.

The variation is taken on a fixed void shape. For example, the family of ellipses are characterized by the shape parameter $m$. For any given shape, $\Pi$ can be evaluated as a function of the rate, $\dot{m}$. The latter is then determined to minimize $\Pi$, i.e. by setting $\partial\Pi / \partial\dot{m} = 0$. The shape parameter $m$ is updated for a small time step, and the process repeats itself.

Figure 3 shows the shape evolution. An unstable void collapses to a slit within two units of the characteristic time, which is 74 h at 500 K for a void of initial radius of 0.3 $\mu$m.

## INSTABILITY UNDER ELECTRIC CURRENT

Figure 4 illustrates a cylindrical void in an infinite conductor subjected to a remote electric field in the $x$-direction, $E$. On the void surface, the electric field only has the tangential component, $E_t$. The electron wind exerts a force on each atom on the void surface:

$$F^* = -Z_s^* e E_t, \tag{7}$$

where $Z_s^*$ (> 0) the effective valence, and $e$ (> 0) the magnitude of the electron charge. The negative sign means that atoms diffuse in the direction of the electron wind.

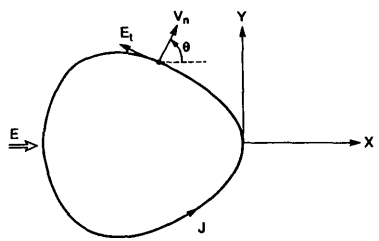


Fig. 4 A void in an infinite conductor under electric field.

In the electron wind, a circular void may undergo a *shape-preserving* migration [10]. A sufficiently large void will break away from a grain boundary or a triple point junction [11]. Based on experimental observations, Kraft *et al.* [4] suggested that the electron wind should amplify certain perturbations from the circular shape, leading to the transgranular slits. We argued that the surface energy will strive to restore the circular shape, and identified a dimensionless ratio [12,13]

$$\chi = \frac{Z_s^* e E a_0^2}{\Omega \gamma_s}. \tag{8}$$

When $\chi$ is small, the surface energy dominates, and the circular void is stable. When $\chi$ is large, the electric field dominates, and a slit will form. A recent calculation, however, showed that the translating circular cavity is *stable* against any *infinitesimal* perturbation [14]. Described in the following is our recent simulation of voids having *finite* perturbations from a circle.

The energy balance, which defines the diffusion driving force $F$, becomes

$$\dot{\Phi} + \int FJdl = \int F^* Jdl. \tag{9}$$

The last term is the power supplied by the electron wind to the surface, and $\Phi$ is the surface energy. Equations (3) and (5) are still valid. The corresponding functional becomes

$$\Pi = \dot{\Phi} + \int \left( \frac{J^2}{2M} - F^* J \right) dl. \tag{10}$$

To capture current crowding around the void, we conformally mapped the exterior of a unit circle on the $\zeta$-plane, $\zeta = \exp(i\theta)$, to the exterior of the void on the $z$-plane:

$$z = A\zeta + B + \sum_{n=1}^{\infty} C_n \zeta^{-n}. \tag{11}$$

The coefficients $A$, $B$ and $C_i$ were evolved according to the variational principle (10). We took finite terms in (11) in the numerical simulations. The electric potential on the void surface is $\phi = -2AE\cos\theta$, and the tangential electric field $E_t = -\partial\phi / \partial l$.

Figure 5a shows the evolution of voids starting with the same shape but subjected to different levels of $\chi$. The time between two consecutive snapshots is $0.233 a_0^4 / \left(\Omega^2 M \gamma_s\right)$, so the relative position along the $x$-axis gives the average migration velocity during this time period. At a low field level, $\chi = 5$, the void relaxes to a circle. At a high field level, $\chi = 15$, the void collapses to a slit. The critical level seems to lie between $10 < \chi_c < 11$. Under $E$ = 500 V/m, the critical void radius is $a_0 \approx 0.3$ $\mu$m. Once the void becomes unstable, it quickly collapses to a slit, often in much less than one unit of the characteristic time. Since the void is stable against any infinitesimal perturbation [14], the critical condition obtained here depends on the magnitude of the finite perturbation used in the simulation.

Figure 5b shows voids starting from different shapes but under the same field level, $\chi = 20$. The time between two snapshots is $0.14 a_0^4 / \left(\Omega^2 M \gamma_s\right)$. Even a void elongated along the line direction, which is not fatal to the line, will evolve to a slit across the line causing fatal failure. In all cases, the voids adjust their shapes so that the side facing the electron wind becomes flat. Once the voids reach this condition, they quickly elongate across the line, and their migration along the line slows down. The same features have been observed experimentally by Kraft *et al.* [4].

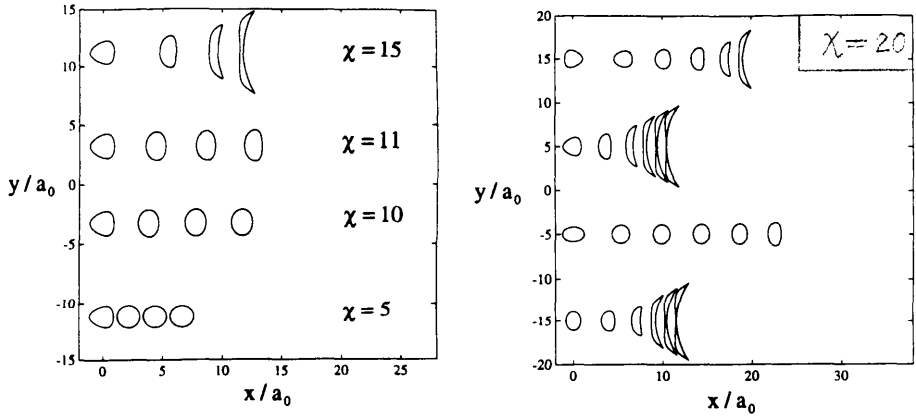


Fig. 5 a) Void evolution under different electric field. b) Voids of different initial shapes under the same electric field. The remote electric field is directed from the left to the right.

## CONCLUSION

A sufficiently large void in an interconnect will collapse to a transgranular slit due to diffusion along the void surface. The instability is an outcome of the competition of the surface energy with the thermal stress (1), or with the electric current (8). The model is two dimensional and the void is assumed to be in an infinite, isotropic grain. Removal of these idealizations will not alter the essential picture, but will change numerical values. Once the void reaches the critical size, it collapses to a slit quickly. Consequently, an interconnect is likely to spend most of its lifetime in growing a rounded void to a critical size. Further attention should be directed toward nucleation and growth of rounded void, so that the major portion of the lifetime can be predicted.

**Acknowledgments**—The work was supported by the NSF through grant MSS-9202165, and a Young Investigator Award MSS-9258115 to ZS. THH was in part supported by the NSFC.

## REFERENCES

1. J. E. Sanchez, L. T. McKnelly, and J. W. Morris, J. Appl. Phys. **72**, 3201 (1992).
2. J. H. Rose, Appl. Phys. Lett. **61**, 2170 (1992).
3. Y.-C. Joo and C. V. Thompson, Mater. Res. Soc. Symp. Proc. **309**,351 (1993).
4. O. Kraft, S. Bader, J. E. Sanchez and E. Arzt, Mater. Res. Symp. Proc. **309**, 199 (1993).
5. C.V. Thompson and J.R. Lloyd, MRS Bulletin, December Issue, p. 19 (1993).
6. F.H. Wohlbier, *Diffusion and Defect Data—Solid State Data*, Vol. 47 (Trans Tech Publications, Switzerland, 1986).
7. H. Gao, Q. J. Mech. Appl. Math. **45**, 149 (1992).
8. Z. Suo and W. Wang, submitted to J. Appl. Phys. (1994).
9. M.A. Korhonen, unpublished work.
10. P.S. Ho, J. Appl. Phys. **41**, 64 (1970).
11. C.-Y. Li, P. Borgesen, and M.A. Korhonen, Appl. Phys. Lett. **61**, 411 (1992).
12. Z. Suo, W. Wang and M. Yang, Appl. Phys. Lett. **64** (15) (1994).
13. W. Yang, W. Wang and Z. Suo, J. Mech. Phys. Solids. (in press).
14. M. Marder, unpublished work.